ANL/TD/CP--85125
Conf-9409107--4

RELATIVE PERFORMANCE PROPERTIES OF THE ORNL ADVANCED NEUTRON SOURCE REACTOR WITH REDUCED ENRICHMENT FUELS*

M. M. Bretscher, J. R. Deen, N. A. Hanan, J. E. Matos, S. C. Mo
R. B. Pond, A. Travelli, and W. L. Woodruff
Argonne National Laboratory
Argonne, IL USA

To be presented at the
1994 International Meeting on
Reduced Enrichment for Research and Test Reactors

September 18-23, 1994
Williamsburg, Virginia, USA

The submitted manuscript has been authored by a contractor of the U. S. Government under contract No. W-31-109-ENG-38. Accordingly, the U. S. Government retains a nonexclusive, royalty-free license to publish or reproduce the published form of this contribution, or allow others to do so, for U. S. Government purposes.

DISCLAIMER

This report was prepared as an account of work sponsored by an agency of the United States Government. Neither the United States Government nor any agency thereof, nor any of their employees, makes any warranty, express or implied, or assumes any legal liability or responsibility for the accuracy, completeness, or usefulness of any information, apparatus, product, or process disclosed, or represents that its use would not infringe privately owned rights. Reference herein to any specific commercial product, process, or service by trade name, trademark, manufacturer, or otherwise does not necessarily constitute or imply its endorsement, recommendation, or favoring by the United States Government or any agency thereof. The views and opinions of authors expressed herein do not necessarily state or reflect those of the United States Government or any agency thereof.

*Work supported by the U.S. Department of Energy
Office of Nonproliferation and National Security
under Contract No. W-31-109-38-ENG

MASTER

DISTRIBUTION OF THIS DOCUMENT IS UNLIMITED

DISCLAIMER

Portions of this document may be illegible in electronic image products. Images are produced from the best available original document.

RELATIVE PERFORMANCE PROPERTIES OF THE ORNL ADVANCED NEUTRON SOURCE REACTOR WITH REDUCED ENRICHMENT FUELS

M. M. Bretscher, J. R. Deen, N. A. Hanan, J. E. Matos, S. C. Mo,
R. B. Pond, A. Travelli, and W. L. Woodruff

Argonne National Laboratory
Argonne, Illinois 60439 USA

ABSTRACT

Three cores for the Advanced Neutron Source reactor, differing in size, enrichment, and uranium density in the fuel meat, have been analyzed. Performance properties of the reduced enrichment cores are compared with those of the HEU reference configuration. Core lifetime estimates suggest that none of these configurations will operate for the design goal of 17 days at 330 MW. With modest increases in fuel density and/or enrichment, however, the operating lifetimes of the HEU and MEU designs can be extended to the desired length. Achieving this lifetime with LEU fuel in any of the three studied cores, however, will require the successful development of denser fuels and/or structural materials with thermal neutron absorption cross sections substantially less than that of Al-6061. Relative to the HEU reference case, the peak thermal neutron flux in cores with reduced enrichment will be diminished by about 25-30%.

INTRODUCTION

The Advanced Neutron Source (ANS) is a very high performance nuclear research reactor being designed at the Oak Ridge National Laboratory (ORNL). Operating under steady state conditions, the ANS reactor is intended to provide a neutron flux at experiment locations which is at least five times higher than that available at any existing facility.

The ANL RERTR Program was commissioned[1] to evaluate performance characteristics of ANS cores with fuel of reduced enrichment. This study focuses on the neutronic properties of three cores differing in size, enrichment, and uranium density in the fuel meat. Performance properties of a 108.2 liter LEU core (20.0 wt % ^{235}U, 4.8 g U/cm^3) and a 82.6 liter MEU core (35.0 wt % ^{235}U, 3.5 g U/cm^3) are compared with those of the 67.6 liter HEU reference core (93.2 wt % ^{235}U, 1.7 g U/cm^3). To meet desired operational requirements, the reference core is designed to operate for 17 full power days (FPD) at a fission power of 330 MW. Larger core volumes and higher fuel densities are needed in the MEU and LEU designs to match this reference cycle length and power level. Consequently, cores with fuel of reduced enrichment will have lower thermal neutron fluxes at the experiment locations.

GEOMETRIC MODELS OF THE ANS REACTOR

Geometric models and material compositions used in this study were supplied by ANS personnel[2] at both ORNL and the Idaho National Engineering Laboratory (INEL). Alternate core designs, significantly different from those proposed by ORNL, were not evaluated in this study.

Figures 1-3 show RZ models (not to scale) of the heavy water-moderated and -reflected ANS reactor. The HEU 67.6 liter core uses two fuel elements while the lower enrichment cores need three fuel elements. Natural hafnium rods control the reactor. These figures do not show the hafnium shutdown

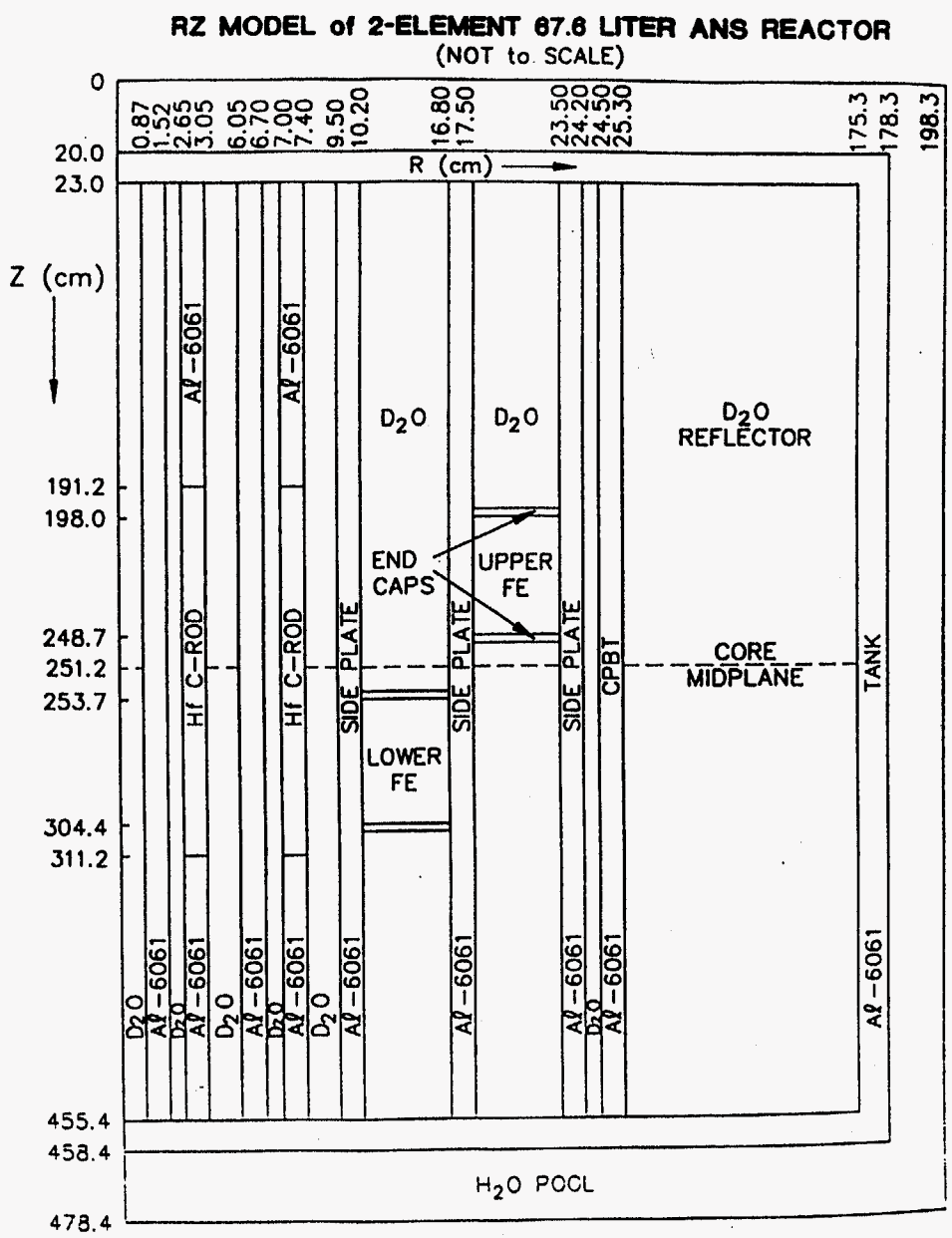

Figure 1

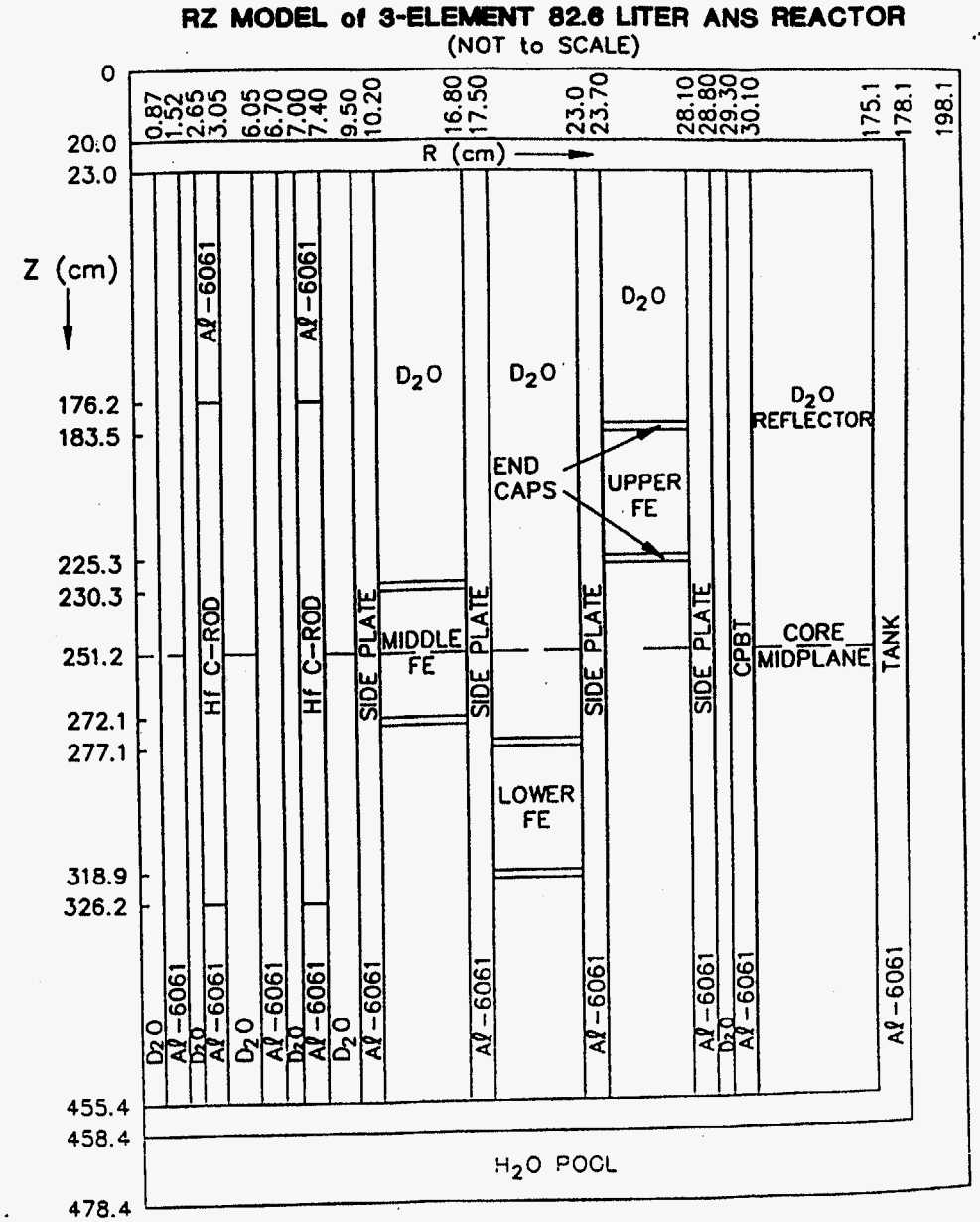

Figure 2

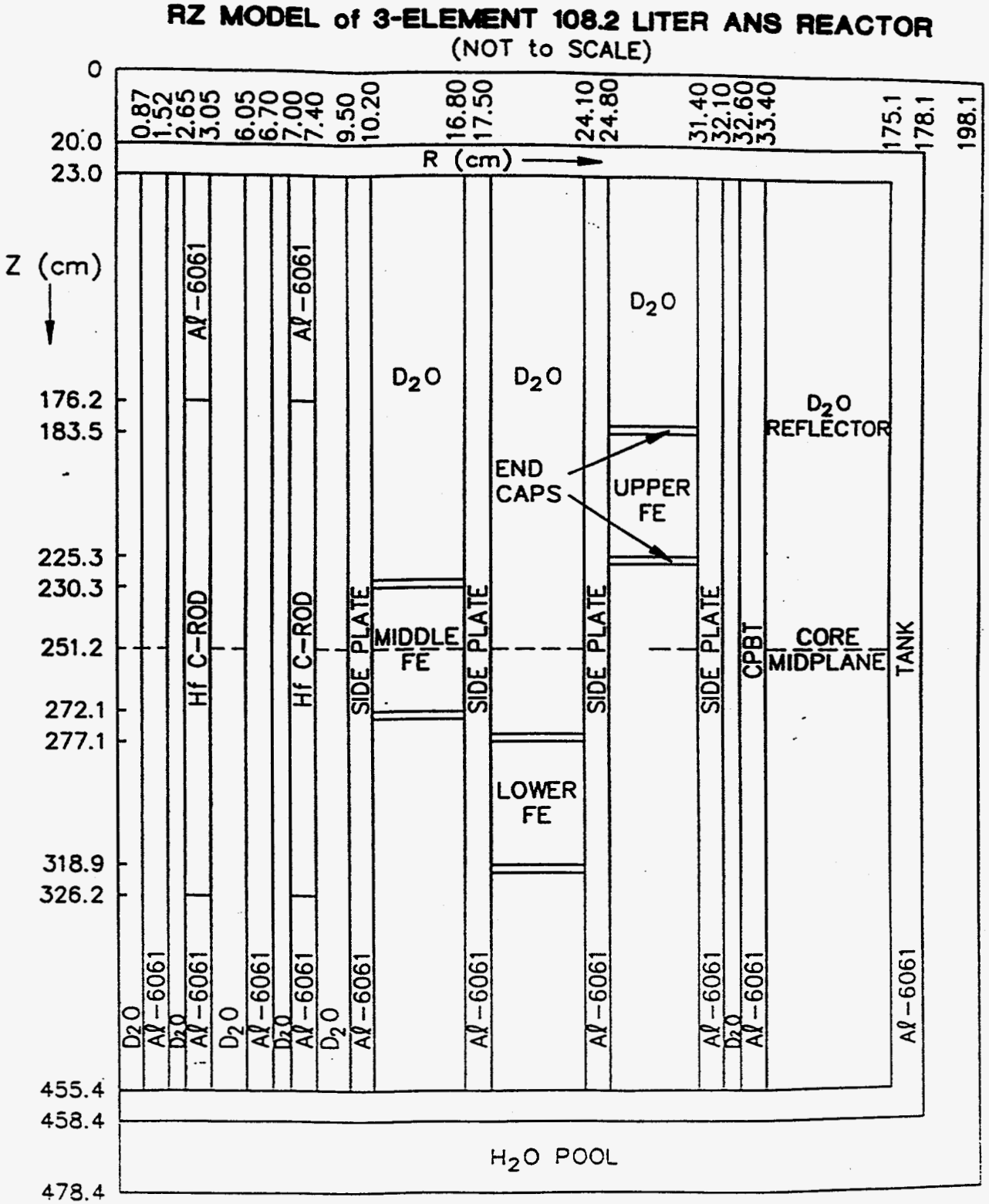
RZ MODEL of 3-ELEMENT 108.2 LITER ANS REACTOR
(NOT to SCALE)
R (cm)
Z (cm)
0
20.0
23.0
176.2
183.5
225.3
230.3
251.2
272.1
277.1
318.9
326.2
455.4
458.4
478.4
0.87
1.52
2.65
3.05
6.05
6.70
7.00
7.40
9.50
10.20
16.80
17.50
24.10
24.80
31.40
32.10
32.60
33.40
175.1
178.1
198.1
Aℓ-6061
Hf C-ROD
D2O
MIDDLE FE
SIDE PLATE
END CAPS
UPPER FE
LOWER FE
D2O REFLECTOR
CPBT
CORE MIDPLANE
TANK
H2O POOL

Figure 3

rods, the internal irradiation targets, nor the components (beam tubes, targets, hot and cold sources, etc.) in the D_2O radial reflector.

Fuel plates and coolant channels are of equal thickness (0.127 cm) and follow the path of an involute from the inner to the outer circular side plate of the fuel element. The fuel meat consists of U_3Si_2 particles dispersed in aluminum. For the HEU reference design, the meat thickness varies in both the axial and radial directions. This fuel "grading" is designed to minimize power peaking effects. A filler of 1100 aluminum powder is used to maintain a constant plate thickness. The meat-filler combination is clad with Al-6061 plates 0.0254 cm thick.

If the total ^{235}U content in the core is fixed, the neutron multiplication factor and the neutron flux at experiment positions are quite insensitive to meat thickness variations. For these neutronic calculations, therefore, the meat thickness was assumed to be uniform for the MEU and LEU fuel elements. In an actual core design, fuel grading probably would be necessary and so a uniform aluminum filler of the same volume used in the HEU plates was added to the fuel plates of reduced enrichment. However, this filler volume has not been optimized.

Figure 4 shows a sketch of the reflector components in the axial midplane of an ANS 3-element core. This complicated geometry can only be roughly approximated in an RZ model. Monte Carlo methods with generalized 3D geometry descriptions are best suited to describe the effects of the reflector components.

Figure 4 also shows the cluster of three hafnium control rods at the center of the reactor. For 2-dimensional RZ calculations these rods are replaced with two concentric rods (see Figs. 1-3) whose radii and spacing were carefully chosen so as to match the reactivity worth of the actual 3-rod cluster and not distort the power shape.

Table 1 provides a summary of the fuel element properties for the three ANS cores analyzed in this study. Some characteristics of the involute-shaped fuel plates are given in Table 2. Region-dependent atom densities are shown in Table 3. Note that the heavy water is assumed to contain a light water impurity of 0.25 atom %.

The composition of the end cap regions above and below the fuel (see Figs. 1-3) was assumed to be a 50/50 volume percent mixture of Al-6061 and heavy water. In an actual fuel element design, it may be necessary to assign a burnable poison to this region to hold down the initial reactivity and to reduce power peaking. For these analyses, however, the burnable poison was omitted.

COMPUTATIONAL METHODS

Our neutronic analyses of the ANS cores depend on a combination of continuous energy Monte Carlo and finite difference multigroup diffusion theory calculations. Because of its very generalized three-dimensional capability, the Monte Carlo neutron/photon-coupled MCNP code[3] can best describe the complicated geometries of the reflector components (see Fig. 4). For fuel cycle analyses, however, the REBUS code[4], with DIF3D[5] fluxes, was used for fuel depletion studies. This code package uses burnup-dependent multigroup cross sections correlated with ^{235}U depletion.

Multigroup Cross Sections

Multigroup cross sections were generated with the WIMS-D4M code[6] together with a new 69-group library[7]. As for MCNP, the cross section library is based on ENDF/B-V data. In the ANS fuel regions the neutron spectrum is strongly influenced by neutrons scattered back into the fuel by the surrounding heavy water. Therefore, a large cylindrical cell duplicating a radial slice through the ANS reactor in the horizontal plane of one of the fuel elements was used in WIMS. By flux-weighting cross

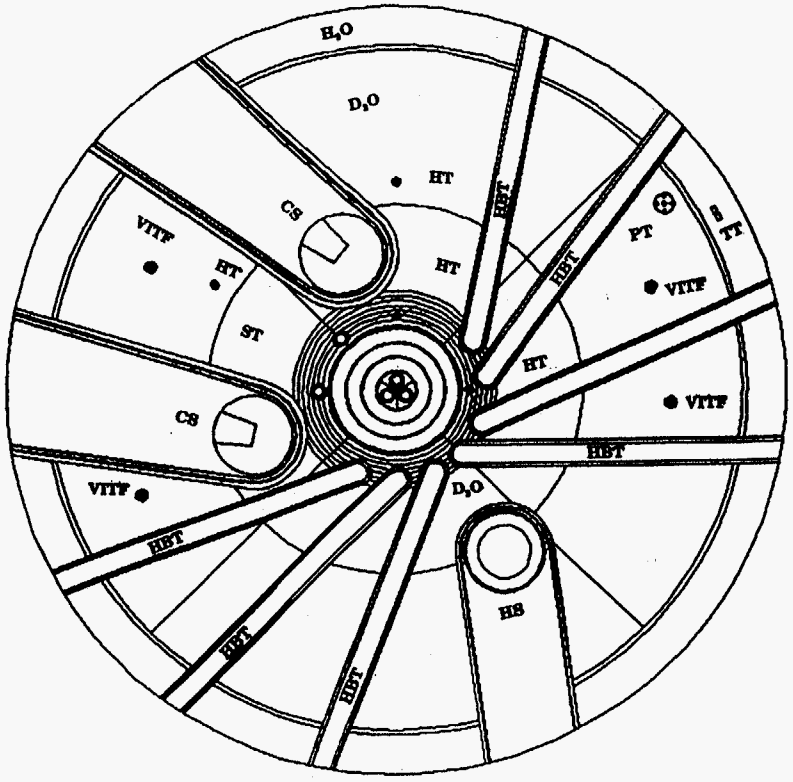

Figure 4
Reflector Components in the Horizontal Midplane of the ANS 3-Element Core

Definitions
CS ≡ cold source
HBT ≡ horizontal beam tube
HS ≡ hot source
HT ≡ hydraulic tube
PT ≡ pneumatic tube
ST ≡ slant tube
TT ≡ transfer tube
VITF ≡ vertical isotope target facility

TABLE 1
ANS FUEL ELEMENT PROPERTIES

Property	HEU Core	MEU Core	LEU Core
Isotopic Enrichment (wt. %)			
^{234}U	1.053	0.364	0.199
^{235}U	93.200	35.000	20.000
^{236}U	0.429	0.161	0.092
^{238}U	5.318	64.475	79.709
U Density in Fuel Meat (g/cm^3)	1.7	3.5	4.8
Fuel Plate Thickness (cm)	0.127	0.127	0.127
Coolant Channel Thickness (cm)	0.127	0.127	0.127
Thickness of Side Plates (cm)	0.70	0.70	0.70
Active Height of Fuel (cm)	50.7	41.8	41.8
Number of Fuel Elements	2	3	3
Inner/Outer Radii of Fuel Zones (cm)			
Upper Fuel Element	17.5/23.5	23.7/28.1	24.8/31.4
Middle Fuel Element	--	10.2/16.8	10.2/16.8
Lower Fuel Element	10.2/16.8	17.5/23.0	17.5/24.1
Core Volume (liters)			
Upper Fuel Element	39.2	29.9	48.7
Middle Fuel Element	--	23.4	23.4
Lower Fuel Element	28.4	29.3	36.1
Total	67.6	82.6	108.2
Fuel Plates Per Element			
Upper Fuel Element	433	586	613
Middle Fuel Element	--	252	252
Lower Fuel Element	252	433	433
Initial ^{235}U Mass (kg)			
Upper Fuel Element	14.78	8.64	11.62
Middle Fuel Element	--	6.76	5.59
Lower Fuel Element	8.93	8.45	8.60
Total	23.71	23.85	25.81
Average Fuel Meat Thickness (cm)	0.0563	0.0599	0.0632

TABLE 2
PROPERTIES OF INVOLUTE-SHAPED FUEL PLATES
(DISTANCES IN CM AND ANGLES IN RADIANS)

Core Volume (liters)	Parameter*	Upper Fuel Element	Middle Fuel Element	Lower Fuel Element
67.6	s	7.029	--	8.735
	θ	0.896	--	1.309
	dθ/ds	0.064	--	0.075
82.6	s	4.808	8.735	6.364
	θ	0.637	1.309	0.853
	dθ/ds	0.066	0.075	0.067
108.2	s	7.478	8.735	7.845
	θ	0.603	1.309	0.947
	dθ/ds	0.052	0.075	0.060

*s is the length of the involute path from the inner to the outer side plate and θ is the angle subtended by s with respect to the radial center of the circular side plates. dθ/ds is a rough index of the stiffness of the fuel plates and increases with increasing rigidity.

From the parametric equations for the involute of a circle, it follows that

$$s = \frac{a}{2}\left[\frac{b^2}{a^2} - 1\right], \quad \theta = \left[\frac{b^2}{a^2} - 1\right]^{1/2}, \text{ and } \quad d\theta/ds = (b^2 - a^2)^{-1/2}$$

where a and b are the inner and outer radii of the annular fuel zone, respectively.

TABLE 3
REGION-DEPENDENT ATOM DENSITIES
(in units of atoms/barn-cm)

Element or Isotope	Control Rods	Al-6061 Alloy	Homogenized Fuel		
			HEU 1.7 gU/cm^{3b}	MEU 3.5 gU/cm^3	LEU 4.8 gU/cm^3
H			8.1622-5	8.1622-5	8.1622-5
D			3.2567-2	3.2567-2	3.2567-2
O-16			1.6324-2	1.6324-2	1.6324-2
Mg		6.6871-4	1.3374-4	1.3374-4	1.3374-4
Al		5.8220-2	2.7101-2	2.5045-2	2.0360-2
Si		3.4722-4	8.9510-4	1.5261-3	2.1371-3
Cr		6.2517-5	1.2504-5	1.2504-5	1.2504-5
Mn		4.4377-5	1.2717-5	1.2206-5	1.1713-5
Fe[a]		3.5352-4	1.1132-4	1.0590-4	1.0069-4
Cu		7.6072-5	2.1803-5	2.0924-5	2.0078-5
Hf	4.4773-2				
^{234}U			1.2034-5	7.7368-6	6.1004-6
^{235}U			1.0604-3	7.4000-4	6.1146-4
^{236}U			4.8572-6	3.3896-6	2.8008-6
^{238}U			5.9744-5	1.3460-3	2.4062-3

Isotope	Light and Heavy Water			
	H_2O	D_2O Near C-Rods	D_2O Near FE's	D_2O Radial Refl.
H	6.6633-2	1.6618-4	1.6236-4	1.6604-4
D		6.6310-2	6.4784-2	6.6236-2
O-16	3.3316-2	3.3236-2	3.2482-2	3.3199-2

[a] Scaled to account for neutron absorption in the trace quantities of Ti and Zn present in Al-6061.

[b] Atom densities correspond to the maximum meat thickness in the graded HEU fuel.

sections over distinct annular regions, multigroup cross sections were obtained not only for the homogenized fuel ring, but also for each H_2O, D_2O, Al-6061, and Hf region. In order to make the cross sections less dependent on neutron spectrum changes, a structure of 15 energy groups was adopted. Burnup-dependent cross sections were generated for the fuel region and complete cross section sets were prepared for each fuel enrichment. Explicit fission product cross sections were generated for ^{135}Xe and ^{149}Sm together with their precursors ^{135}I and ^{149}Pm. A lumped fission product cross section was created to represent the combined effect of all the remaining fission products. The burnup behavior of the lumped fission products is discussed in a separate paper[8] at this conference. At the beginning-of-cycle (BOC) the WIMS-generated cross sections were found to compare very favorably with those calculated by the MCNP and VIM[9] Monte Carlo codes. Table 4 illustrates this comparison for some uranium cross sections. WIMS and VIM results are for identical cells, but MCNP is for a 3D model of the reactor with cross sections collapsed over a single fuel element.

Fuel cross sections were generated using a homogenized mixture of fuel meat (including the aluminum filler), cladding material, and heavy water in the annular fuel ring of the WIMS cylindrical cell model. In reality, however, the fuel element region is a heterogeneous succession of involute-shaped fuel meat, clad, and heavy water channels. Monte Carlo calculations were performed to estimate the importance of these heterogeneous effects. Table 5 illustrates some of these results for the case of ^{238}U capture in the LEU fuel elements. The general conclusion is that the hard spectrum in the fuel region makes heterogeniety effects unimportant.

Hafnium Control Rods

Natural hafnium is a strong neutron absorber with large capture resonances in the 1-12 eV energy range. Because of the large absorption cross sections in groups 9-15, steep flux gradients occur near the hafnium surfaces. These steep gradients violate the conditions under which diffusion theory is valid. Therefore, special methods are needed for treating hafnium control rods in diffusion theory calculations. For groups 1-8 the hafnium capture cross sections are small enough so that normal diffusion theory can be applied.

The method used in this study treats hafnium as a non-diffusing medium for groups 9-15 by applying a group-dependent internal boundary condition at the hafnium surfaces. This internal boundary condition is the neutron current-to-flux ratio. Beginning with the same cylindrical model used to generate the WIMS cross sections, but with a much finer mesh within and about the hafnium rods, P_1S_{16} transport calculations were used to determine numerical values for the internal boundary conditions. For a few groups, these values were too large and thus were replaced by values corresponding to the limiting case of a "black" rod of the same radius. Figure 5, derived from data in Ref. 10, is a plot of the radius-dependent black boundary condition.

Table 6 compares BOC MCNP integral rod worths for the 2-ring model with corresponding REBUS/DIF3D values based on the use of internal boundary conditions. Within 1σ statistics both methods give the same values for the Hf control rod worths. For the purpose of these calculations, the "rods out" condition was taken to be that with the hafnium (Figs. 1-3) replaced by Al-6061.

Reflector Component Worths

The reactivity worth of the reflector components severely limits the cycle lengths of the ANS cores. Because of the complicated geometry of these components (Fig. 4), they are best described by the generalized 3D treatment in MCNP. However, approximate RZ models of the reflector components have been developed by the ORNL group[2] for use in their VENTURE-diffusion code. We have used MCNP as well as REBUS/DIF3D (with ORNL's RZ models) to calculate the worth of the reflector components at both beginning-of-cycle (BOC) and at end-of-cycle (EOC). With the control rods withdrawn and parked in the upper reflector at EOC, REBUS EOC atom densities were used in the MCNP Monte Carlo

TABLE 4
MICROSCOPIC CROSS SECTION RATIOS FOR LEU FUEL
Hf CONTROL RODS WITHDRAWN
(LOWER FUEL ELEMENT)

Group	E_L - eV	$^{235}U(n,f)$		$^{238}U(n,\gamma)$	
		WIMS/VIM[a]	WIMS/MCNP[b]	WIMS/VIM[a]	WIMS/MCNP[c]
1	8.21+5	1.000	1.012	1.004	0.996
2	6.73+4	1.000	1.001	1.000	1.000
3	1.50+4	0.995	0.996	1.014	1.002
4	5.53+3	1.001	0.998	1.009	0.958
5	1.43+3	1.002	0.997	0.964	0.929
6	3.67+2	1.003	0.978	0.930	0.937
7	2.77+1	0.981	0.945	0.895	0.881
8	9.88	0.999	1.003	0.976	0.969
9	4.00	0.931	0.945	0.939	0.979
10	1.04	0.974	0.996	0.996	0.996
11	0.625	1.002	1.001	1.000	0.998
12	0.300	1.014	1.018	1.003	1.003
13	0.180	0.998	0.999	1.006	1.006
14	0.042	1.023	1.014	1.018	1.008
15	1.0-5	0.998	0.999	1.002	0.997

[a] The 1σ statistics are <<1% for all groups.
[b] The 1σ statistics are <2% for all groups.
[c] The 1σ statistics are <3.2% for all groups.

TABLE 5
$^{238}U(n,\gamma)$ HOMOGENEOUS/HETEROGENEOUS CROSS SECTION RATIOS IN THE ANS LEU CORE

Group	E_L - eV	Homogeneous/Heterogeneous Ratio	
		VIM (Cell)[a]	MCNP (Middle FE)[b]
1	8.21+5	0.977	0.974
2	6.73+4	0.993	0.993
3	1.50+4	1.002	1.000
4	5.53+3	1.032	1.000
5	1.43+3	1.004	1.014
6	3.67+2	1.010	1.031
7	2.77+1	1.028	1.016
8	9.88	1.031	1.071
9	4.00	1.034	1.044
10	1.04	1.002	1.004
11	0.625	1.005	1.004
12	0.300	1.012	1.009
13	0.180	1.015	1.017
14	0.042	1.019	1.022
15	1.0-5	1.037	1.033

[a] Statistical error of 1σ <1.4% for all groups.
[b] Statistical error of 1σ <5.8% for all groups.

INTERNAL BOUNDARY CONDITIONS FOR BLACK CONTROL RODS

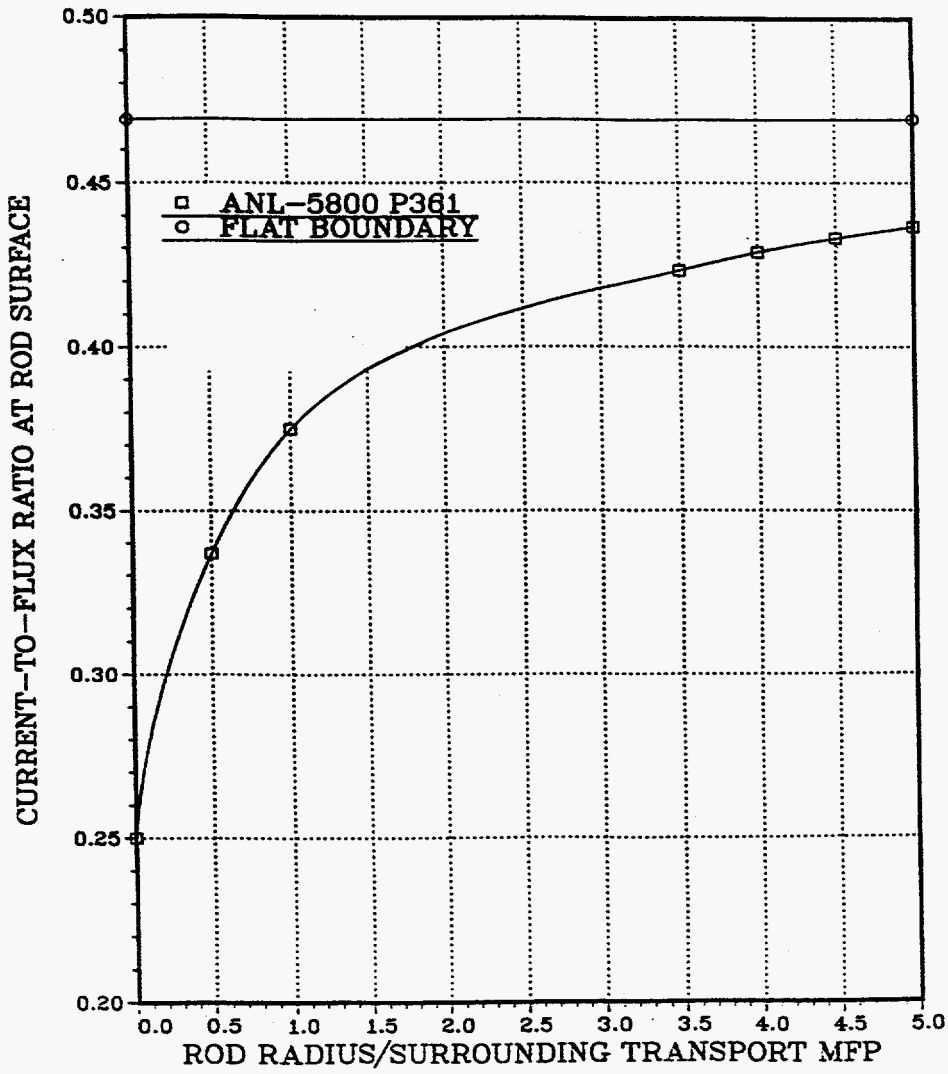

Figure 5

TABLE 6
INTEGRAL WORTHS IN % $\delta k/k^2$ OF THE ANS HAFNIUM CONTROL RODS AT BOC

Core	With Refl. Components ?	DIF3D Diffusion	MCNP Monte Carlo
67.6L HEU	No	-14.01	-14.27±0.20
1.7 gU/cm^3	Yes	-17.58[a]	-17.01±0.23
82.6L MEU	No	-14.15	-14.16±0.23
3.5 gU/cm^3	Yes		-16.35±0.27
108.2L LEU	No	-12.88	-13.03±0.26
4.8 gU/cm^3	Yes		-14.75±0.29

[a] This calculation uses the ORNL-VENTURE RZ model of the reflector components.

calculation. The neutron absorption effect of all the fission products not present in the ANL MCNP library was represented in terms of equivalent, region-dependent, ^{10}B concentrations. Each fuel element was divided into a 3x3 array of equal-volume regions. As a first approximation, the ^{10}B concentrations were chosen to match the combined thermal neutron absorption rates of ^{135}I, ^{135}Xe, ^{149}Pm, and the lumped fission products. These region-dependent ^{10}B concentrations were scaled until a diffusion calculation gave the same eigenvalue as the original EOC REBUS calculation. The EOC MCNP Monte Carlo calculation used these equivalent ^{10}B number densities together with the other EOC atom densities from REBUS.

Table 7 summarizes the results for the reactivity worths of the ANS reflector components. Note that relative to the 3D MCNP calculations, the RZ diffusion model for the HEU reference case overpredicts the worth of the reflector components by nearly 3% $\delta k/k^2$. It appears that the ORNL VENTURE model for the reflectror components is incorrect for the HEU case. The MCNP calculations show that the worth of the reflector components at EOC with the control rods withdrawn is smaller but nearly equal to the BOC value with the control rods fully inserted. This useful result allows the extrapolation of MCNP BOC reflector component worth calculations to EOC conditions.

ANALYTICAL RESULTS

This section presents the results obtained from REBUS/DIF3D diffusion and MCNP Monte Carlo calculations for the three ANS cores studied. Emphasis is placed on eigenvalues, peak thermal neutron fluxes, and core lifetime comparisons.

BOC DIF3D/MCNP Comparisons

Table 8 compares diffusion theory and Monte Carlo results for BOC eigenvalues and peak thermal neutron fluxes for each of the ANS models analyzed in this study. The reflector components are included in some of the MCNP models, but not in the DIF3D calculations. For the purpose of these comparisons, the control rod "out" configuration corresponds to the inserted Hf rods (Figs. 1-3) replaced with Al-6061. In reality, however, the fully withdrawn control rods are parked in the upper reflector with the bottom of the hafnium located on the plane where the top of the hafnium would be for a fully inserted rod. Figures 1-3 show the control rods in the fully inserted position. Table 8 shows that the BOC DIF3D eigenvalues are consistently larger than the corresponding MCNP values by an amount of the order of 1% $\delta k/k^2$.

The peak thermal neutron flux is a function of control rod elevation and is largest for fully inserted rods. However, the product of the flux and the eigenvalue is rather insensitive to control rod elevation and fuel burnup. Since the reactor would operate at an effective multiplication factor of unity, this product is a realistic estimate of the peak thermal neutron flux. Table 8 shows that these products for the MCNP calculations are about 1% higher than the corresponding DIF3D values. Relative to the HEU reference core, the Monte Carlo "rods in" unperturbed peak fluxes (i.e. those without the reflector components modeled) for the MEU and LEU cores are reduced by factors of 0.74 and 0.69, respectively. The reflector components perturb the BOC fluxes and lower them by about 20% relative to the corresponding unperturbed values. Figure 6 is a plot of the BOC unperturbed DIF3D thermal neutron flux distributions on the axial midplane of the three cores in the radial reflector outside the core pressure boundary tube (CPBT).

EOC Properties of the Three ANS Cores

A design objective for the ANS is that it operate for 17 days at 330 MW before refueling. Some calculated characteristics at the end of 17 FPD for the ANS cores analyzed in this study are summarized in Table 9. For the REBUS depletion calculations, the reflector components were not modeled and the

TABLE 7
REACTIVITY WORTHS OF THE ANS REFLECTOR COMPONENTS

Core	FPD[a]	Control Rod Position	Worth of Reflector Components in % $\delta k/k^2$	
			REBUS/DIF3D[b]	MCNP
67.6 Liter HEU	0.0	Fully Out	-8.30	-5.13±0.18
1.7g U/cm^3	0.0	Fully In		-7.86±0.25
	17.0	Fully Out	-10.28	-7.50±0.27
82.6 Liter MEU	0.0	Fully Out	-4.74	-4.45±0.20
3.5 g U/cm^3	0.0	Fully In		-6.65±0.30
	17.0	Fully Out	-5.56	
108.2 Liter LEU	0.0	Fully Out	-4.44	-4.92±0.22
4.8g U/cm^3	0.0	Fully In		-6.64±0.32
	17.0	Fully Out	-5.15	-6.38±0.31

[a] All cores were assumed to operate for 17.0 full power days (FPD) at 330 MW.

[b] Based on ORNL RZ models of the reflector components used in their VENTURE diffusion code.

TABLE 8
BOC DIF3D/MCNP EIGENVALUE AND PEAK THERMAL NEUTRON FLUX COMPARISONS

Core	C-Rods	Code	With Refl. Comp.'s ?	Eigenvalue k_{eff}	Peak Flux[a] E+15 n/cm^2-s	Product k_{eff}*Flux
67.6L HEU	Out	DIF3D	No	1.2927	5.16	6.67
1.7 gU/cm^3	Out	MCNP	No	1.2800±0.0020	5.29±0.06	6.77±0.08
	Out	MCNP	Yes	1.2012±0.0019	4.50±0.09	5.41±0.10
	In	DIF3D	No	1.0945	6.18	6.77
	In	MCNP	No	1.0823±0.0019	6.29±0.08	6.81±0.08
	In	MCNP	Yes	0.9974±0.0019	5.55±0.11	5.53±0.11
82.6L MEU	Out	DIF3D	No	1.2438	4.02	5.00
3.5 gU/cm^3	Out	MCNP	No	1.2234±0.0020	4.13±0.05	5.06±0.06
	Out	MCNP	Yes	1.1602±0.0020	3.32±0.08	3.85±0.09
	In	DIF3D	No	1.0577	4.82	5.10
	In	MCNP	No	1.0428±0.0020	4.86±0.05	5.07±0.06
	In	MCNP	Yes	0.9752±0.0022	4.23±0.10	4.12±0.10
108.2L LEU	Out	DIF3D	No	1.2204	3.65	4.45
4.8 gU/cm^3	Out	MCNP	No	1.2056±0.0023	3.71±0.05	4.48±0.06
	Out	MCNP	Yes	1.1381±0.0021	3.23±0.08	3.67±0.09
	In	DIF3D	No	1.0546	4.46	4.70
	In	MCNP	No	1.0419±0.0022	4.53±0.06	4.72±0.06
	In	MCNP	Yes	0.9745±0.0023	4.35±0.09	4.24±0.09

[a] The peak flux is for neutrons with energies below 0.625 eV and for a power of 330 MW. MCNP statistics are the 1σ values.

ANS UNPERTURBED MIDPLANE THERMAL NEUTRON FLUX DIST.

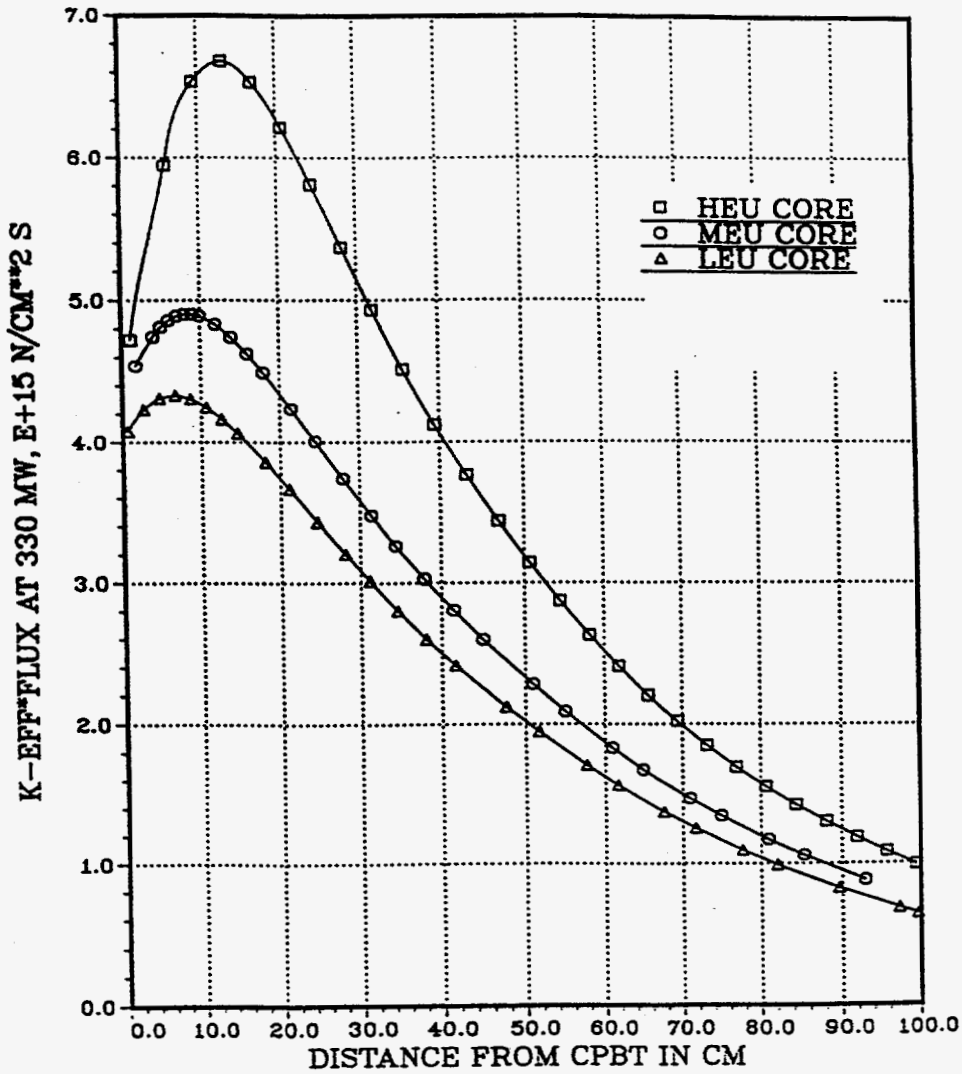

Figure 6

TABLE 9
PROPERTIES OF ANS CORES AT THE END OF 17 FULL POWER DAYS
(CONTROL RODS WITHDRAWN, P = 330 MW)

Core	Code	With Refl. Comp's ?	Eigenvalue k_{eff}	Peak Flux E+15n/cm²-s	Product k_{eff}*Flux	% ^{235}U Burnup	Pu Mass g
67.6L HEU 1.7 gU/cm³	REBUS	No	1.0981	6.18	6.79	30.9	46.9
	MCNP	No	1.0945±0.0025	6.62±0.13	7.25±0.14		
	MCNP	Yes	1.0115±0.0018	5.56±0.11	5.62±0.11		
82.6L MEU 3.5 gU/cm³	REBUS	No	1.0620	4.70	5.03	29.7	369.6
108.2L LEU 4.8 gU/cm³	REBUS	No	1.0570	4.21	4.44	27.0	644.1
	MCNP	No	1.0492±0.0021	4.83±0.11	5.07±0.12		
	MCNP	Yes	0.9834±0.0024	3.73±0.08	3.67±0.08		

reactor was allowed to operate for 17 days at 330 MW with the control rods fully withdrawn. Like the results given earlier at BOC, Table 9 shows that after 17 FPD the peak unperturbed flux is significantly degraded for the MEU and LEU cores relative to the HEU reference and that the reflector components further reduce the peak flux compared with the unperturbed values. The EOC flux ratios are comparable to the BOC values discussed earlier.

Maximum core lifetime estimates have been made using the EOC reactivity balance table shown in Table 10. This table was constructed from data given in Tables 7-9. Normally, a reactivity reserve would be included in this table. This reserve is needed to overcome the buildup of ^{135}Xe and restart the reactor within a short time after an unanticipated shutdown. This balance table determines the minimum unperturbed multiplication factor needed at EOC from which the maximum core lifetime can be found. Figure 7 shows how these lifetime estimates were obtained. The estimated maximum core life for the 67.2 liter HEU, the 82.6 liter MEU, and the 108.2 liter LEU core is 17.0, 15.4, and 12.3 days, respectively, at 330 MW.

Three-Element 108.2 Liter LEU Overlap Core

In recent ANS internal progress reports[11] it was stated that increased peak thermal neutron fluxes and core reactivities would result if the upper fuel element were lowered to be even with the middle fuel element (see Fig. 3). We have analyzed this "overlapping" core configuration for the 108.2 liter LEU case.

With the control rods fully inserted, BOC MCNP Monte Carlo calculations showed that the peak unperturbed thermal neutron flux for this overlap core increased by a factor of 1.052 relative to the normal configuration. The corresponding flux ratio from REBUS/DIF3D calculations was 1.055. For the MCNP perturbed calculations the peak flux for the overlap core decreased by a factor of 0.968 relative to the non-overlap configuration. An estimate of the lifetime of this overlap core was determined, as described earlier, on the basis of an EOC reactivity balance table. The MCNP-calculated worth of the reflector components at BOC is 8.42 ± 0.19 % $\delta k/k^2$. Using results in Table 7 as a guide for extrapolation, the EOC worth of the reflector components for this overlap configuration was estimated to be 8.09% $\delta k/k^2$. Including an EOC REBUS bias factor of 0.68% $\delta k/k^2$, the required excess reactivity at EOC for the unperturbed REBUS calculation is 8.77% $\delta k/k^2$. This translates into a required EOC eigenvalue of 1.0961. Figure 8 shows the unperturbed eigenvalues as a function of exposure in FPD as well as core lifetime estimates for the normal and overlap configurations for the 108.2 liter LEU core. This figure indicates that no significant improvement in core life results from the overlap configuration. The increased worth of the reflector components offsets the advantages of larger eigenvalues for the overlap core.

Sensitivity of Lifetime and Performance to the Choice of Structural Material

For the ANS cores a significant reactivity loss is associated with parasitic neutron capture in the Al-6061 structural materials. Sizeable reactivity gains would be achieved if some or all of the Al-6061 could be replaced with a material significantly less absorbing to neutrons. To investigate the potential effects of this type of substitution, some calculations were performed with magnesium replacing Al-6061 in some or all of the structures of selected ANS cores.

The results show that dramatic improvements would result if substitutions of this type were feasible. For example, substitution of all structural materials (excluding fuel plates) in the LEU 108.2 liter core with 4.8 g U/cm^3 would increase the reactivity available after 17 days at 330 MW by approximately 12% $\delta k/k^2$, which could be used to increase the core lifetime from 12.3 to 36.2 days. The peak thermal neutron flux would also increase 15%, from 4.4 to 5.1 x 10^{15} n/cm^2 s. Similar results were obtained for other ANS cores. In particular, for the 82.6 liter core, substitution of magnesium for Al-6061 in all structural materials yielded a 13% $\delta k/k^2$ increase in reactivity at EOC. Substitution for individual

TABLE 10
REACTIVITY BALANCE TABLE AT THE END OF 17 FPD[a]
(CONTROL RODS WITHDRAWN)

Reactivity Component	Reactivity Worth (% $\delta k/k^2$)		
	67.6 Liter HEU 1.7g U/cm^3	82.6 Liter MEU 3.5g U/cm^3	108.2 Liter LEU 4.8g U/cm^3
Reflector Components	7.50	6.34	6.38
DIF3D Bias (Relative to MCNP)	0.30	0.50	0.70
Total, ρ	7.80	6.84	7.08
Required EOC k-eff $= (1-\rho)^{-1}$	1.0846	1.0734	1.0762

[a] This balance table assumes:

1. The control rods are parked in the upper reflector.
2. The H_2O contamination in D_2O is 0.25 atom %.
3. The worth of the reflector components is based on MCNP Monte Carlo calculations.
4. DIF3D bias factors (relative to MCNP) are included.

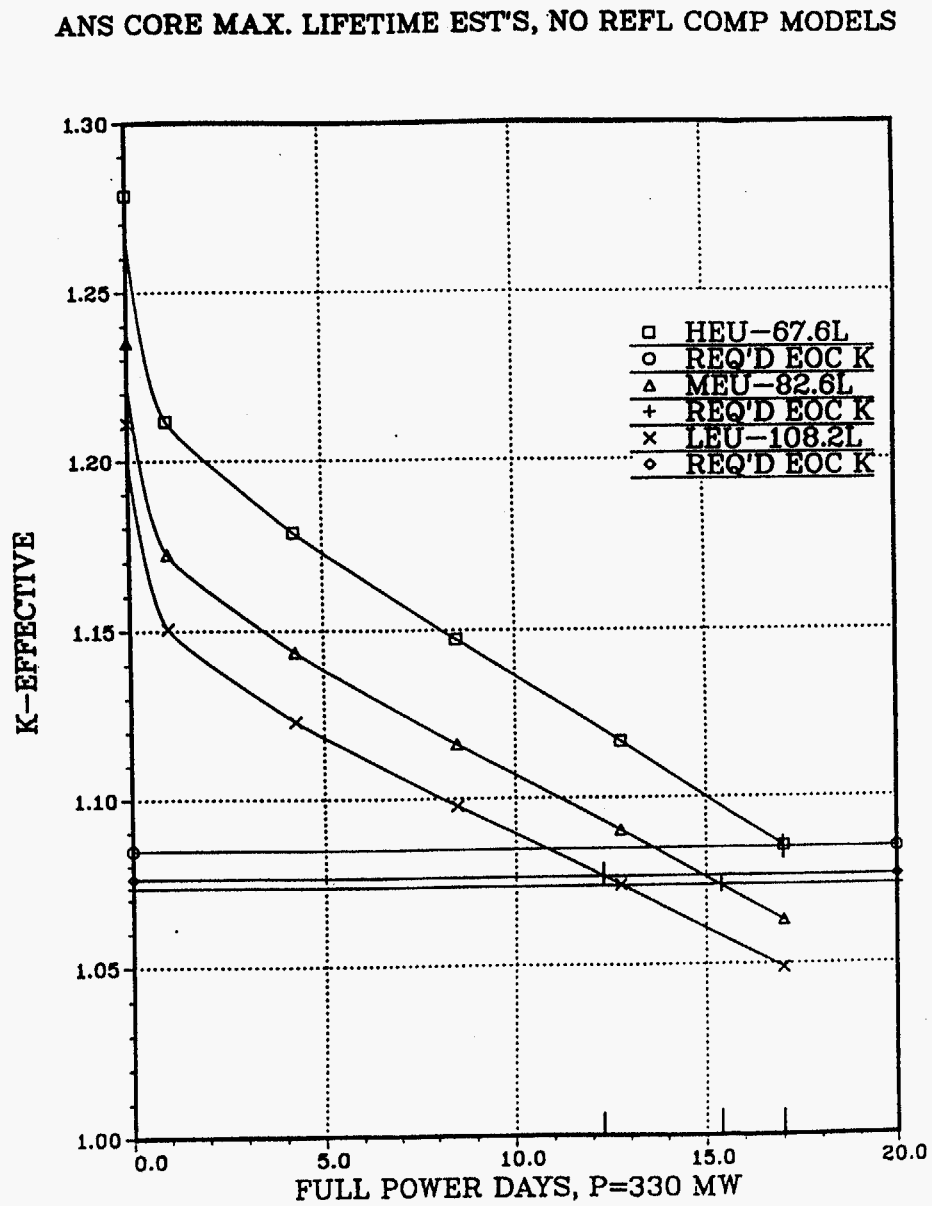

Figure 7

ANS MAX. LIFETIME EST'S FOR 108.2 LITER LEU CORES

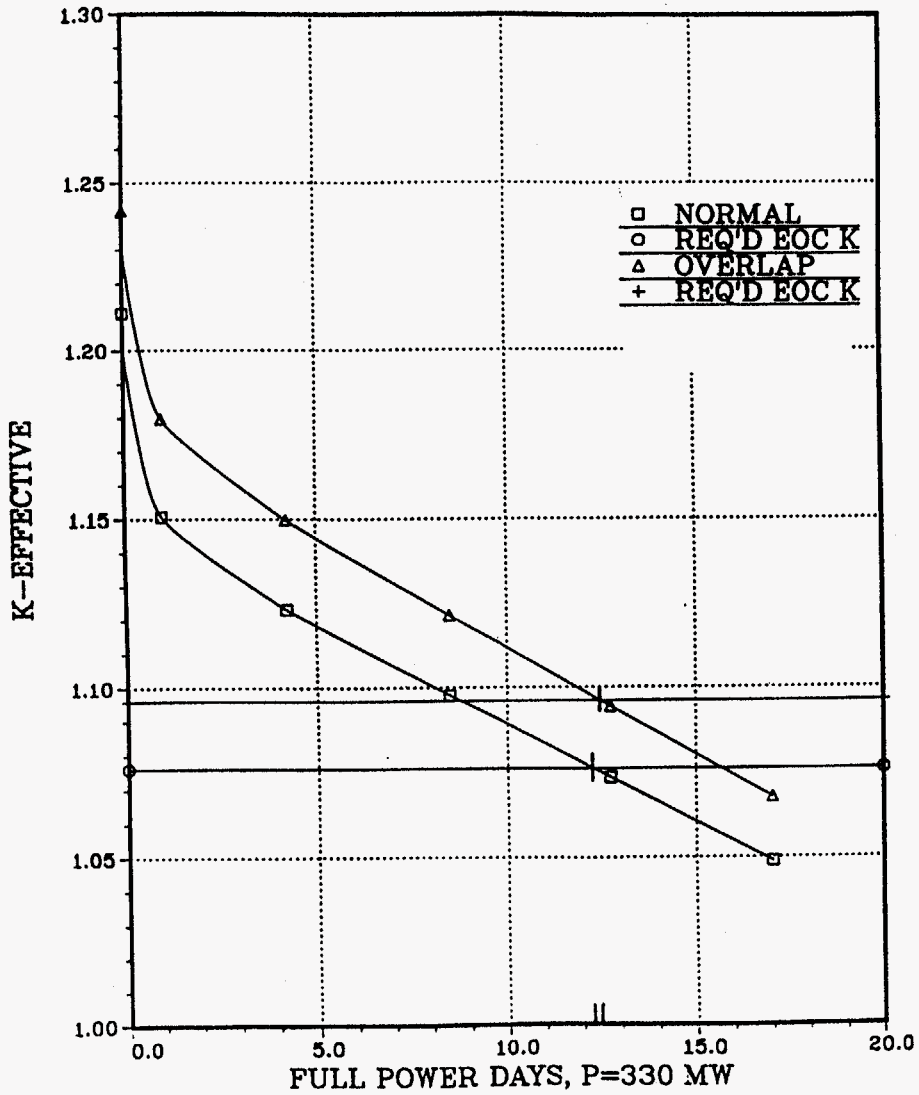

Figure 8

TABLE 11
CORE LIFETIME ESTIMATES AND BOC MCNP PEAK THERMAL NEUTRON FLUKES RELATIVE TO THE UNPERTURBED HEU REFERENCE CORE FOR FULLY INSERTED CONTROL RODS

Core	Lifetime	Relative Peak Thermal Neutron Flux	
	FPD[a]	No Reflector Comp's	With Reflector Comp's
67.6 Liter HEU 1.7g U/cm^3	17.05	1.00[b]	0.81
82.6 Liter MEU 3.5g U/cm^3	15.35	0.74	0.60
108.2 Liter LEU 4.8g U/cm^3	12.30	0.69	0.62
108.2 Liter LEU 4.8g U/cm^3 (overlay case)	12.48	0.75	0.61

[a] FPD = Days at 330 MW.

[b] The peak thermal neutron flux for the unperturbed HEU reference core was 6.81E+15 n/cm^2-sec.

structural components contribute to this total in the following percentages: fuel element side plates (50%), core pressure boundary tube (27%), reflector components (13%), and control rod followers and tubes (10%). Thus, the effect of using structural materials other than Al-6061 even in structures which will be present in the ANS core for only short periods of time, like the fuel element side plates, would be very significant.

These considerations address only the neutronic effects of the substitution. Whether high magnesium content alloys are available or can be developed to withstand the harsh environment of an ANS core is of fundamental importance, but is an issue not addressed in this study.

CONCLUSIONS

Peak thermal neutron fluxes relative to the unperturbed HEU reference core, as well as lifetime estimates for the three ANS cores analyzed in this study, are summarized in Table 11. This table illustrates the size of neutron flux penalties associated with the use of larger volume cores required by fuels of reduced enrichment and also flux reductions caused by the reflector components. Since the reactivity balance tables, upon which the core lifetime estimates are based, do not include allowances for in-core target facilities nor for any operational reserves, it is unlikely that any of these cores will operate for 17 days at 330 MW of fission power. However, the uranium density for the HEU core could be increased to offset these additional reactivity requirements. Similarly, the 82.6 liter MEU core design could be modified by increasing the enrichment and/or the fuel density so that it too could operate for 17 full power days.

However, design improvements will be needed for obtaining substantial reactivity additions before the 108.2 liter LEU core could operate for the desired cycle length at 330 MW. Our calculations indicate that the maximum power density in the LEU core is about one half that in the HEU reference. This suggests that perhaps some of the aluminum filler assigned to the LEU fuel plates is not needed and could be replaced with additional fuel meat. Carefully placed burnable poisons will help limit initial power peaking values. But it seems likely that this LEU core design will require the development and certification of higher density fuels with improved thermal conductivities. Large reactivity additions are also possible if structural materials with significantly less parasitic absorption for thermal neutrons than Al-6061 can be developed for use in the fuel side plates and/or other ANS structures. Otherwise, the LEU core will have to operate for a shorter cycle and/or a lower power level.

Several important issues have not been addressed by this study. Table 2 shows that for these three core designs the fuel plates in the upper element of the LEU core are the least stable. Whether these plates are mechanically stable under the high coolant flow rates required to maintain centerline meat temperatures at acceptable levels for the high density, low thermal conductivity, LEU fuel is of central importance but beyond the scope of this study. To reduce power peaking effects it is assumed that, like the HEU reference core, the LEU fuel will need to be graded in both the axial and radial directions. Whether the high density LEU fuel can be graded and fabricated with acceptable yields is another important issue outside the scope of this study.

REFERENCES

1. Communication from Edward Fei, Director, International and Regional Security Division, Office of Nonproliferation and National Security, U.S. Department of Energy and Robert A. Bari, Department of Nuclear Energy, Brookhaven National Laboratory, September 1993.

2. J. P. Renier and J. C. Gehin of the ORNL Reactor Physics Analysis Group provided input streams for their VENTURE depletion code used to analyze several ANS configurations. C. A. Wemple from INEL gave similar information for use with the MCNP Monte Carlo code. This information allowed us to carry out this study using ANS models consistent with theirs.

3. "Documentation for CCC-200/MCNP 4.2 Code Package", RSIC Computer Code Collection, Oak Ridge National Laboratory, September 1993.

4. B. J. Toppel, "A User's Guide for the REBUS-3 Fuel Cycle Analysis Capability", ANL-83-2, March 1983.

5. K. L. Derstine, "DIF3D: A Code to Solve One-, Two-, and Three-Dimensional Finite-Difference Diffusion Theory Problems," Argonne National Laboratory Report ANL-82-64, April 1984.

6. C. I. Costescu, D. G. Cacuci, J. R. Deen, and W. L. Woodruff, "Microscopic Cross Sections for and from the WIMS-D4 Cell Code," Trans. Amer. Nucl. Soc. 68, 471 (1993).

7. J. R. Deen, W. L. Woodruff, and C. I. Costescu, "New ENDF/B-V Nuclear Data Library for WIMS-D4M," 16th International RERTR Meeting, Oarai, Ibaraki, Japan, October 3-7, 1993.

8. S. C. Mo, "Methodology and Application of the WIMS-D4M Fission Product Data," 17th International RERTR Meeting, Williamsburg, Virginia, USA, September 18-23, 1994.

9. R. Blomquist, "VIM-A Continuous Energy Neutronics and Photon Transport Code," ANS Proceedings of the Topical Meeting on Advances in Reactor Computations, Salt Lake City, Utah, pp. 222-224, March 1983.

10. L. J. Templin, Ed., "Reactor Physics Constants", 2nd edition, pp. 361-363, ANL-5800, July 1963.

11. F. Gallmeier, et al., Oak Ridge National Laboratory, unpublished information (June 1994).